analytical chemistry

pubs.acs.org/ac

Letter

Rapid Classification of COVID-19 Severity by ATR-FTIR Spectroscopy of Plasma Samples

Arghya Banerjee, Abhiram Gokhale, Renuka Bankar, Viswanthram Palanivel, Akanksha Salkar, Harley Robinson, Jayanthi S. Shastri, Sachee Agrawal, Gunter Hartel, Michelle M. Hill,* and Sanjeeva Srivastava*

Cite This: *Anal. Chem.* 2021, 93, 10391−10396

Read Online

ACCESS | Metrics & More | Article Recommendations | Supporting Information

ABSTRACT: The coronavirus disease 2019 (COVID-19) pandemic continues to ravage the world, with many hospitals overwhelmed by the large number of patients presenting during major outbreaks. A rapid triage for COVID-19 patient requiring hospitalization and intensive care is urgently needed. Age and comorbidities have been associated with a higher risk of severe COVID-19 but are not sufficient to triage patients. Here, we investigated the potential of attenuated total reflectance Fourier-transform infrared (ATR-FTIR) spectroscopy as a rapid blood test for classification of COVID-19 disease severity using a cohort of 160 COVID-19 patients. A simple plasma processing and ATR-FTIR data acquisition procedure was established using 75% ethanol for viral inactivation. Next, partial least-squares-discriminant analysis (PLS-DA) models were developed and tested using data from 130 and 30 patients, respectively. Addition of the ATR-FTIR spectra to the clinical parameters (age, sex, diabetes mellitus, and hypertension) increased the area under the ROC curve (C-statistics) for both the training and test data sets, from 69.3% (95% CI 59.8−78.9%) to 85.7% (78.6−92.8%) and 77.8% (61.3−94.4%) to 85.1% (71.3−98.8%), respectively. The independent test set achieved 69.2% specificity (42.4−87.3%) and 94.1% sensitivity (73.0−99.0%). Diabetes mellitus was the strongest predictor in the model, followed by FTIR regions 1020−1090 and 1588−1592 cm^{-1}. In summary, this study demonstrates the potential of ATR-FTIR spectroscopy as a rapid, low-cost COVID-19 severity triage tool to facilitate COVID-19 patient management during an outbreak.

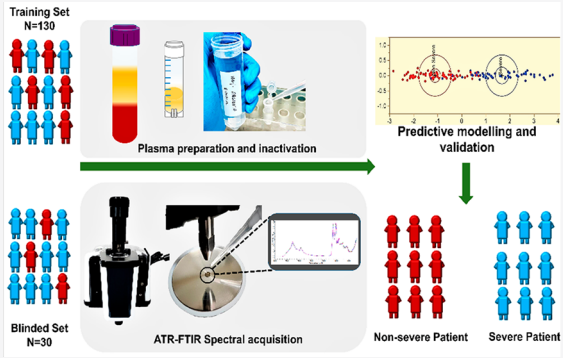

At the end of 2019, humankind faced one of the most significant ongoing threats in the form of Severe Acute Respiratory Syndrome Coronavirus 2 (SARS-CoV-2). After rapidly spreading throughout the world, the World Health Organization (WHO) declared COVID-19 (coronavirus disease 2019) to be a global pandemic on March 11, 2020.[1] The initial symptoms of COVID-19 include fever, dry cough, and strenuous breathing. Despite global public health measures, the spread of SARS-CoV-2 has continued throughout the world, with more than 157 million infections recorded[2] as of May 8, 2021. The recent emergence of SARS-CoV-2 mutations with higher infection rates[3] may further overwhelm the already overburdened healthcare infrastructure, causing shortages of intensive care unit (ICU) beds, oxygen ventilators, and medical staff.

While some patients suffer mild symptoms and recover, around one in five patients requires intensive care for pneumonia with acute respiratory distress syndrome (ARDS). Risk factors for severe COVID-19 have been identified, including older age, heart diseases, cancer, and diabetes.[4,5] However, these comorbidities/risk factors are not sufficient to predict disease severity, and several clinical measures have been investigated to predict COVID-19 severity, including chest X-ray, MRI, serum biochemistry and proteomics, WBC count, lymphocyte count, creatinine level, bilirubin levels, D-dimer, and C-reactive protein.[6,7] While these additional clinical tests show promise, a simple, rapid test at the point of patient admission would transform hospital management during crises.

Attenuated total reflectance Fourier-transform infrared (ATR-FTIR) spectroscopy is a rapid chemical measurement technique, which has been deployed with a multivariate statistical model for the classification of diseases. Two recent studies reported the potential of ATR-FTIR as a rapid screening test for COVID-19 using plasma[8] or nasopharyngeal swab.[9] Given the reported blood biochemistry changes in severe COVID-19 disease,[6,7] we hypothesized that ATR-FTIR

Received: February 8, 2021
Accepted: June 29, 2021
Published: July 19, 2021

https://doi.org/10.1021/acs.analchem.1c00596
Anal. Chem. 2021, 93, 10391−10396

spectra of plasma samples would differentiate between severe and non-severe disease. Herein, we developed a predictive algorithm for COVID-19 disease stratification into severe and non-severe COVID-19 using ATR-FTIR spectra, in addition to clinical variables that are available to the physician at the point of admission.

EXPERIMENTAL SECTION

Participants and Samples. All plasma samples were collected with approval from the Institute Ethics Committee, IIT Bombay, and Kasturba Hospital for Infectious Diseases, Institutional Review Board. Experiments were performed as per Institutional Review Board guidelines, following policies and regulations for the involvement of human subjects.

Blood was collected in an EDTA vacutainer from confirmed and suspected individuals who visited Kasturba Hospital, Bombay, following infection control protocol approved by the World Health Organization (WHO) and Indian Council of Medical Research (ICMR). Plasma was isolated by centrifuging blood at 10 000 rpm for 5 min. Plasma samples left over after clinical diagnostic use were aliquoted into cryovials (~1 mL) stored at −80 °C.

The severity of cases was defined by O_2 saturation less than 90% observation and other clinical complications such as bilateral pneumonia and/or ground-glass opacity, and/or has bilateral crests or have acute respiratory distress syndrome.

Plasma Sample Processing and ATR-FTIR Spectral Acquisition. Plasma was thawed on ice, and a 100 μL aliquot was added to a sterile tube containing 300 μL chilled absolute ethanol (Merck) and vortexed briefly. Ethanol-treated plasma samples were stored at −20 °C until spectral acquisition. For acquisition, samples were thawed on ice and each sample was vortexed before 1 μL was placed on the crystal and allowed to dry.

FTIR spectra were measured within the 4000 to 650 cm^{-1} wavenumber regions using a Cary 630 (Agilent) spectrometer coupled with the ATR module. The ATR detection diamond was cleaned with 100% v/v ethanol and background spectra were acquired before every acquisition. A 1 μL portion of the sample was placed on the ATR crystal and air-dried (approximately 30 s). Background and sample spectra were acquired at a spectral resolution of 8 cm^{-1} with 64 scans per measurement. The instrument parameters are apodization Happ Genzel, phase correction Mertz, and set method gain 218. Sample spectra were recorded in technical duplicates.

Statistical Analysis and Algorithm Development. FTIR spectra were exported for analysis using JMP Pro (version 15.2.1). Regions 4000−3701 cm^{-1} were removed as initial studies established that this region tended to have variable background without distinct peaks. Technical duplicates were averaged. For each data set, spectra were normalized by the area under the curve (AUC) using the formula $AUC_{sample}/AUC_{average\ for\ data\ set}$. Smoothing used a 9-point Savitzky−Golay filter. Partial least-squares-discriminant analysis (PLS-DA) was used with a NIPALS fit. The number of factors was set to four based on leave one out cross-validation. Age was entered as a continuous variable while sex, hypertension, and diabetes mellitus were entered as discrete variables. Variable importance scores were calculated and plotted with a stringent cutoff of 1. Contingency analysis was used to calculate sensitivity and specificity.

RESULTS

Sample Preparation Method Development. A simple, standardized method was established for ATR-FTIR spectra acquisition using the Cary 630, which also complies with biosafety procedures.[10−12] Prepared plasma samples (in 75% ethanol v/v) was vortexed and then 1 μL was deposited on the ATR crystal and allowed to dry before spectra acquisition using set parameters as stated in the Experimental Section. The reproducibility of FTIR spectra acquired using this method was confirmed by acquiring spectra of the same sample multiple times and by three different research analysts (data not shown). During this study, ethanol-inactivated plasma samples were incubated at −20 °C overnight. However, the freezing step is not necessary and incubation at −20 °C for 0, 4, 8 h, and overnight produced similar results (Figure S1).

FTIR Spectra Acquisition. Plasma samples from 160 clinicopathologically confirmed SARS-CoV-2 patients (positive for E, ORF, RdRp, and N genes by RT-PCR) were procured from Kasturba Hospital, Mumbai, and randomly divided into two cohorts based on the time of data acquisition. There were 130 samples in the training set for predictive model development and 30 samples in the blind testing set (Table S1). As a quality control step, correlation analysis between the two cohorts reported $r = 0.99$ for Pearson pairwise group correlation (Figure S2).

The severity of cases was revealed from clinical data after FTIR data acquisition (Table 1). Severe patients were significantly older than non-severe patients and enriched for the comorbidities of hypertension and diabetes mellitus. There was no difference between sex in the two groups.

Table 1. Participant Characteristics

Training set		Severe	Non-severe
number		52	78
age (years)	median range	58.5 (32−77)	50.5 (22−79)
sex	male	33 (63%)	54 (59%)
comorbidities	hypertension	25 (48%)	25 (32%)
	diabetes mellitus	25 (48%)	14 (17%)
Blind test set		**Severe**	**Non-severe**
number		17	13
age (years)	median range	63 (40−80)	45 (18−69)
sex	male	12 (71%)	9 (70%)
comorbidities	hypertension	8 (47%)	2 (15%)
	diabetes mellitus	7 (41%)	2 (15%)

Predictive Model Development. For model development, technical duplicate spectra were averaged for each sample, and then spectra for the 130 training samples were normalized by AUC. Full clinical data could not be obtained for two patients and were discarded from further study. In total, 128 samples were used for model building, with the input of age, sex, hypertension, diabetes mellitus, and FTIR spectra. Figure 1a shows the average spectra for the severe and non-severe groups, which are very similar overall and comparable to previous reports of FTIR of plasma and serum.[13,14]

Multivariate statistics using PLS-DA was conducted on the data set, including the clinical parameters age, sex, hypertension, and diabetes mellitus. After leave-one-out cross-validation, the minimum root mean PRESS was 0.874 43 and the minimizing number of factors was 4. Variable importance of the projection (VIP) scores were used to determine the importance of parameters in the model[15] (Figure 1b). VIP

https://doi.org/10.1021/acs.analchem.1c00596
Anal. Chem. 2021, 93, 10391−10396

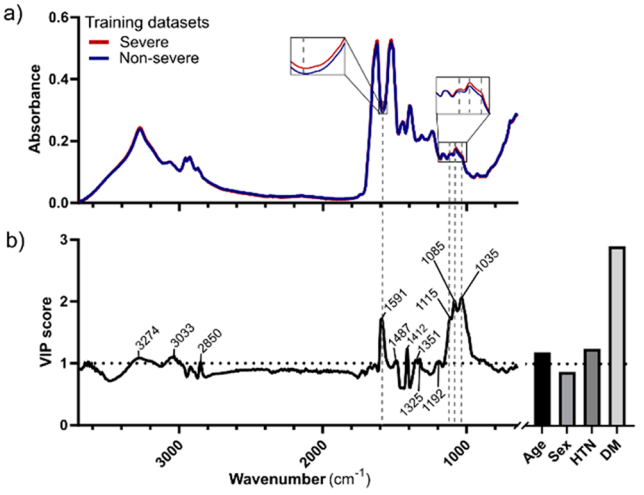

Count	Non-severe	Severe	Total *Actual*
Non-severe	64 65	13 12	77
Severe	26 19	25 32	51
Total *Predicted*	90 84	38 44	128
Sensitivity (95% CI)	**49.0%** (35.0-62.3%) **62.7%** (49-74.7%)		
Specificity (95% CI)	**83.1%** (73.2-89.9%) **84.4%** (74.7-90.9%)		

Figure 1. Developing PLS-DA model for COVID-19 disease severity from plasma ATR-FTIR spectra. (a) Averaged raw spectra for severe (red) and non-severe (blue) groups, with insets showing the two highest scoring VIP regions. Secondary derivatives are shown in Figure S3. (b) VIP plot showing relative contributions of FTIR regions and clinical variables to the predictive model. (c) Receiver operating curve analysis comparing predictive models using clinical parameters alone (age, sex, hypertension, diabetes mellitus) and with the addition of FTIR data. (d) Contingency table for the two models. AUC, under the curve; VIP, variable importance of the projection.

scores combine the variable's contribution to both the response variable (Y) and the latent X factors and denote the relative contribution of the variable (i.e., clinical parameter or specific IR wavelengths) to COVID-19 severity prediction. The strongest predictor for COVID-19 severity was diabetes mellitus with a VIP score of 2.9 (Figure 1b). A comparison of the VIP score plot in Figure 1b with the averaged spectra in Figure 1a shows that the FTIR regions important in distinguishing severe from non-severe COVID-19 are not the highest peaks in the raw spectra. The insets in Figure 1a illustrate the small but observable differences between the average spectra of severe and non-severe COVID-19 groups. The region 1020−1090 cm^{-1} had VIP scores between 1.85 and 2.05 and may correspond to saccharide C−O stretching[16,17] and phosphate (PO_2^-).[9] The second highest FTIR spectral VIP region 1588−1592 cm^{-1} with a VIP score of 1.72 has been described as a primary amine peak (N−H bending).[18] These speculative biological assignments remain to be confirmed experimentally.

Having developed predictive models, we next asked if the use of FTIR spectra improved COVID-19 severity prediction above the clinical parameters alone as assessed by the C-statistic (area under the ROC curve) and cross tabulation of predicted versus actual outcomes (confusion matrix) (Figure 1c, d). The addition of FTIR data improved the C-statistics from 69.3 to 85.7%, primarily driven by the increased sensitivity from 49.0 to 62.7%.

Predictive Model Evaluation. Finally, we evaluated the performance of the predictive model using the 30 independent samples set aside for evaluation. The severity status of these samples was blinded to the researchers acquiring the FTIR spectra and the statistician. We observed visually similar raw average spectra and consistent differences in the two major VIP regions between severe and non-severe groups (Figure 2a inset). The C-statistics and confusion matrix showed that addition of the FTIR data to clinical parameters improved the C-statistic from 77.8 to 85.1%. Sensitivity was improved from 41.2 to 94.1%, but specificity was reduced from 84.6 to 69.2% (Figure 2b, c).

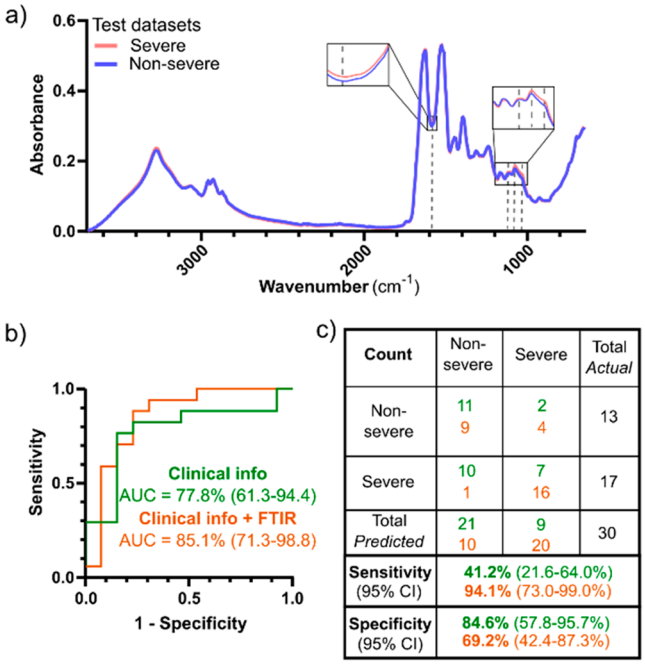

Count	Non-severe	Severe	Total *Actual*
Non-severe	11 9	2 4	13
Severe	10 1	7 16	17
Total *Predicted*	21 10	9 20	30
Sensitivity (95% CI)	**41.2%** (21.6-64.0%) **94.1%** (73.0-99.0%)		
Specificity (95% CI)	**84.6%** (57.8-95.7%) **69.2%** (42.4-87.3%)		

Figure 2. Independent evaluation of the PLS-DA model for COVID-19 disease severity. (a) Averaged raw spectra for the test set, with insets showing the two highest scoring VIP regions. Secondary derivatives are shown in Figure S3. (b) Receiver operating curve analysis. (c) Contingency table. AUC, under the curve; VIP, variable importance of the projection.

DISCUSSION

We report the development of a simple, high sensitivity, virtually reagent-free ATR-FTIR blood test for use in conjunction with existing patient data for first-line COVID-19 triage. The COVID-19 pandemic continues to ravage the world, with infection surges overwhelming health system intensive care resources in many countries globally. The assay developed here aimed to assist frontline physicians in the rapid triaging of diagnosing COVID-19 patients.

The potential of ATR-FTIR as a rapid COVID-19 screening test was recently reported in two papers,[8,9] using serum or nasopharyngeal swab samples. While the same technology was used, the studies asked different research questions (COVID-19 severity prediction versus COVID-19 screening) and used different sample types and statistical models. A further key difference in our study is the sample preparation and data

https://doi.org/10.1021/acs.analchem.1c00596
Anal. Chem. 2021, 93, 10391−10396

acquisition method. To minimize interference from solvent peaks, we acquired spectra after solvents were evaporated from the ATR-FTIR crystal, choosing 75% ethanol as a rapid and practical inactivation and sample preparation. The use of solvent facilitates sample drying on the ATR-FTIR crystal, with the 1 μL sample generally dry within 30 s, compared to the 3−5 min reported by Zhang et al.[8] Zhang and colleagues used heating at 65 °C for 30 min to inactivate samples; the inactivation step was not reported by Barauna et al.[9]

In the study design, an external, double-blind validation cohort was included in the current study and in that of Barauna et al.[9] but not in the work of Zhang et al.[8,9] As the initial training data are used for developing and tuning the multivariate statistics model, having external data evaluation is an important step to establish the performance of an algorithm. Furthermore, our study included the clinical parameters age, sex, diabetes mellitus, and hypertension as well as a broad FTIR spectral range (3500−900 cm^{-1}) in the PLS-DA model, while both Zhang and Barauna[8,9] focused on the fingerprint region. While the strongest FTIR peaks for COVID severity prediction were within the fingerprint region, the regions between 3050 and 3275 cm^{-1} also contributed to the signature in this study.

It is interesting to note the overlap in the selection of the region 1050−1090 cm^{-1} in all three studies, despite the different research question (detection versus severity prediction) and sample types (plasma, serum, swab). Specifically, 1035 and 1080 cm^{-1} had the highest VIP scores for severity prediction in our study, while Zhang et al.[8,9] identified 1050−1100 cm^{-1} in serum for COVID-19 infection and 1041, 1069, and 1084 cm^{-1} were included in the five variables identified by Barauna et al.[9] for COVID-19 detection using swabs. While Barauna et al.[9] assigned these bands to PO_2^- and C−O in nucleic acids and ribose, respectively, Zhang et al.[8,9] attributed the band at 1078 cm^{-1} to phospholipids, as free nucleic acids are low in serum, while phospholipids were reported to be altered in severe COVID-19 patient serum.[19] The exact biological interpretation of these bands requires further experimental confirmation in future studies.

Also interesting is the lack of predictive value in the amide regions in our study. Zhang et al.[8,9] identified 1632 cm^{-1} as potentially indicative of the β-pleated sheet characteristic feature of the immunoglobulin domain, which was previously reported (1631 cm^{-1}) to be elevated in hepatitis B (HBV) and hepatitis C (HCV) viral infected sera.[20] Acute antibody responses were detected in patients infected with SARS-CoV-2,[21] with severe patients likely to show early elevated SARS-CoV-2-specific IgG compared to non-severe patients, albeit with a broad variability.[22] The lack of predictive value of the characteristic immunoglobulin in our cohort may be due to the heterogeneity and time-specific nature of the immunoglobulin response to SARS-CoV-2.[21−23] Future studies should investigate this point by collecting time-series plasma samples and using days from symptom onset as a parameter in the analysis.

The finding that diabetes mellitus had the strongest contribution to the predictive model is in agreement with the epidemiology reports that older age and comorbidities diabetes mellitus and hypertension increase the risk of severe COVID-19.[24] The highest VIP scored FTIR regions may correlate to saccharides, although additional confirmatory experiments will be required. Age, hypertension, and several other FTIR regions also contributed to the developed COVID-19 severity prediction algorithm. Hypertension and diabetes mellitus have been associated with a high risk of cardiovascular complications, including cardiac arrest, thus leading to the fatality of severe patients.[24,25] It has been observed that in addition to extensive dysregulation in amino acid metabolism and energy-related pathways such as mannose metabolism, glutathione dysregulation and its deficiency lead to an increased risk of fatality in severe patients.[26] Future studies integrating FTIR spectral biomarkers with metabolomics may allow a more precise assignment of the VIP FTIR peaks observed in this study.

The strengths of this study include the rapid sample preparation and ATR-FTIR data acquisition methodology and the development of a multivariate algorithm combining ATR-FTIR and clinical data. While there were 128 samples in the training data set, the independent data set comprised only 30 samples. Future studies should increase the sample size to increase the predictive performance.

CONCLUSION

ATR-FTIR is a promising technology for rapid, real-time COVID-19 triaging. The simplicity of the sample preparation and spectral acquisition method developed here can be easily undertaken by clinical laboratory personnel. The multivariate prediction model developed in this study could be implemented on the same data acquisition computer, allowing the rapid return of results to facilitate clinical decision making. The lower cost and robust ATR-FTIR instrumentation is a further advantage compared to more expensive omics or cytokine panel tests, considering that the pandemic likely will persist in both developed and developing countries for the next months to years. The availability of a rapid, simple, and economic COVID-19 patient triaging test will facilitate hospitals to prioritize severe patients in a timely manner, potentially reducing the overall ongoing fatalities from COVID-19.

ASSOCIATED CONTENT

Supporting Information

The Supporting Information is available free of charge at https://pubs.acs.org/doi/10.1021/acs.analchem.1c00596.

Figure S1: Optimization of plasma samples preparation at different time point with incubation at −20 °C in both stacked and overlaid formats. **Figure S2:** Correlation analysis between the cohorts. **Figure S3:** Secondary derivative plot of regions 1200−900 and 1700−1500 cm^{-1}. **Table S1:** Clinical data of non-severe samples n = 78 used for predictive model building. **Table S2:** Clinical data of severe samples n = 52 used for predictive model building. **Table S3:** Clinical data of non-severe samples n = 13 used for testing the model. **Table S4:** Clinical data of severe samples n = 17 used for testing the model (PDF)

AUTHOR INFORMATION

Corresponding Authors

Sanjeeva Srivastava − *Department of Biosciences and Bioengineering, Indian Institute of Technology Bombay, Mumbai 400 076, India;* orcid.org/0000-0002-0651-4438; Email: sanjeeva@iitb.ac.in

Michelle M. Hill − *QIMR Berghofer Medical Research Institute, Herston, QLD 4006, Australia;* orcid.org/0000-

https://doi.org/10.1021/acs.analchem.1c00596
Anal. Chem. 2021, 93, 10391−10396

0003-1134-0951; Email: Michelle.Hill@qimrberghofer.edu.au

Authors

Arghya Banerjee − *Department of Biosciences and Bioengineering, Indian Institute of Technology Bombay, Mumbai 400 076, India;* orcid.org/0000-0002-0043-5827

Abhiram Gokhale − *Department of Biosciences and Bioengineering, Indian Institute of Technology Bombay, Mumbai 400 076, India*

Renuka Bankar − *Department of Biosciences and Bioengineering, Indian Institute of Technology Bombay, Mumbai 400 076, India*

Viswanthram Palanivel − *Department of Biosciences and Bioengineering, Indian Institute of Technology Bombay, Mumbai 400 076, India*

Akanksha Salkar − *Department of Biosciences and Bioengineering, Indian Institute of Technology Bombay, Mumbai 400 076, India*

Harley Robinson − *QIMR Berghofer Medical Research Institute, Herston, QLD 4006, Australia*

Jayanthi S. Shastri − *Kasturba Hospital for Infectious Diseases, Mumbai, Maharashtra 400034, India*

Sachee Agrawal − *Kasturba Hospital for Infectious Diseases, Mumbai, Maharashtra 400034, India*

Gunter Hartel − *QIMR Berghofer Medical Research Institute, Herston, QLD 4006, Australia*

Complete contact information is available at: https://pubs.acs.org/10.1021/acs.analchem.1c00596

Author Contributions

A.B., M.M.H., and S.S. conceived and designed the project. A.B., R.B., V.P., A.S., J.S.S., and S.A. collected samples. A.B., A.G., and R.B. collected FTIR data. H.R. and G.H. analyzed FTIR data. A.B. and M.M.H. drafted the manuscript. G.H. and S.S. edited the manuscript. All authors have given approval to the final version of the manuscript.

Notes

The authors declare no competing financial interest.

Data Repository. FTIR dataset from the study is available at https://doi.org/10.5281/zenodo.4805257.

■ ACKNOWLEDGMENTS

The study was supported through Science and Engineering Research Board (SERB), the Government of India (SB/S1/Covid-2/2020), and a seed grant (RD/0520-IRCCHC0-006) from IRCC, IIT Bombay to S.S. A.B. is supported by a CSIR fellowship, India, for a Ph.D. H.R. is supported by an Australian Government Research Training Program (RTP) Scholarship and QIMR Berghofer Ph.D. Top-Up scholarship. We want to acknowledge Agilent Global and Agilent India for providing us with an FTIR Cary 630, their technical support and assistance; they helped us during instrument parameter optimization. We would like to thank Prof. Ambarish Kunwar from the Department of Biosciences & Bioengineering for fabricating the UV device for sample transport and Prof. Anirban Banerjee for the BSL-2 biosafety aspects.

■ REFERENCES

(1) *WHO. Coronavirus: Events as they happen.* https://www.who.int/emergencies/diseases/novel-coronavirus-2019/events-as-they-happen (accessed September 24, 2020).

(2) *Worldometers:Coronavirus Update (Live) Cases and Deaths from COVID-19 Virus Pandemic.* 2021; https://www.worldometers.info/coronavirus.

(3) *WHO|SARS-CoV-2 Variants/COVID-19-Global.* Disease outbreak news. https://www.who.int/emergencies/disease-outbreak-news/item/2020-DON305.

(4) Toyoshima, Y.; Nemoto, K.; Matsumoto, S.; Nakamura, Y.; Kiyotani, K. *J. Hum. Genet.* **2020**, *65* (12), 1075−1082.

(5) Sanyaolu, A.; Okorie, C.; Marinkovic, A.; Patidar, R.; Younis, K.; Desai, P.; Hosein, Z.; Padda, I.; Mangat, J.; Altaf, M. *SN Compr. Clin. Med.* **2020**, *2* (8), 1069−1076.

(6) An, C.; Lim, H.; Kim, D. W.; Chang, J. H.; Choi, Y. J.; Kim, S. W. *Sci. Rep.* **2020**, *10* (1), 1−11.

(7) Ferrari, D.; Milic, J.; Tonelli, R.; Ghinelli, F.; Meschiari, M.; Volpi, S.; Faltoni, M.; Franceschi, G.; Iadisernia, V.; Yaacoub, D.; Ciusa, G.; Bacca, E.; Rogati, C.; Tutone, M.; Burastero, G.; Raimondi, A.; Menozzi, M.; Franceschini, E.; Cuomo, G.; Corradi, L.; Orlando, G.; Santoro, A.; Digaetano, M.; Puzzolante, C.; Carli, F.; Borghi, V.; Bedini, A.; Fantini, R.; Tabbì, L.; Castaniere, I.; Busani, S.; Clini, E.; Girardis, M.; Sarti, M.; Cossarizza, A.; Mussini, C.; Mandreoli, F.; Missier, P.; Guaraldi, G. *PLoS One* **2020**, *15* (11), No. e0239172.

(8) Zhang, L.; Xiao, M.; Wang, Y.; Peng, S.; Chen, Y.; Zhang, D.; Zhang, D.; Guo, Y.; Wang, X.; Luo, H.; Zhou, Q.; Xu, Y. *Anal. Chem.* **2021**, *93*, 2191.

(9) Barauna, V. G.; Singh, M. N.; Barbosa, L. L.; Marcarini, W. D.; Vassallo, P. F.; Mill, J. G.; Ribeiro-Rodrigues, R.; Campos, L. C. G.; Warnke, P. H.; Martin, F. L. *Anal. Chem.* **2021**, *93*, 2950.

(10) Xiling, G.; Yin, C.; Ling, W.; Xiaosong, W.; Jingjing, F.; Fang, L.; Xiaoyan, Z.; Yiyue, G.; Ying, C.; Lunbiao, C.; Liubo, Z.; Hong, S.; Yan, X. *Sci. Rep.* **2021**, *11* (1), 2418.

(11) Chin, A. W. H.; Chu, J. T. S.; Perera, M. R. A.; Hui, K. P. Y.; Yen, H.-L.; Chan, M. C. W.; Peiris, M.; Poon, L. L. M. *Lancet Microbe* **2020**, *1* (1), No. e10.

(12) Kratzel, A.; Todt, D.; V'kovski, P.; Steiner, S.; Gultom, M.; Thao, T. T. N.; Ebert, N.; Holwerda, M.; Steinmann, J.; Niemeyer, D.; Dijkman, R.; Kampf, G.; Drosten, C.; Steinmann, E.; Thiel, V.; Pfaender, S. *Emerging Infect. Dis.* **2020**, *26* (7), 1592−1595.

(13) Butler, H. J.; Brennan, P. M.; Cameron, J. M.; Finlayson, D.; Hegarty, M. G.; Jenkinson, M. D.; Palmer, D. S.; Smith, B. R.; Baker, M. J. *Nat. Commun.* **2019**, *10* (1), 1−9.

(14) Gajjar, K.; Trevisan, J.; Owens, G.; Keating, P. J.; Wood, N. J.; Stringfellow, H. F.; Martin-Hirsch, P. L.; Martin, F. L. *Analyst* **2013**, *138* (14), 3917−3926.

(15) Wold, S.; Sjöström, M.; Eriksson, L. *Chemom. Intell. Lab. Syst.* **2001**, *58*, 109−130.

(16) Bonnier, F.; Baker, M. J.; Byrne, H. J. *Anal. Methods* **2014**, *6* (14), 5155−5160.

(17) Wang, J.; Kliks, M. M.; Jun, S.; Jackson, M.; Li, Q. X. *J. Food Sci.* **2010**, *75* (2), C208.

(18) Ahmad Daud, N.; Chieng, B.; Ibrahim, N.; Talib, Z.; Muhamad, E.; Abidin, Z. *Nanomaterials* **2017**, *7* (6), 135.

(19) Wu, D.; Shu, T.; Yang, X.; Song, J. X.; Zhang, M.; Yao, C.; Liu, W.; Huang, M.; Yu, Y.; Yang, Q.; Zhu, T.; Xu, J.; Mu, J.; Wang, Y.; Wang, H.; Tang, T.; Ren, Y.; Wu, Y.; Lin, S. H.; Qiu, Y.; Zhang, D. Y.; Shang, Y.; Zhou, X. *Natl. Sci. Rev.* **2020**, *7* (7), 1157−1168.

(20) Roy, S.; Perez-Guaita, D.; Bowden, S.; Heraud, P.; Wood, B. R. *Clin. Spectrosc.* **2019**, *1*, 100001.

(21) Long, Q. X.; Liu, B. Z.; Deng, H. J.; Wu, G. C.; Deng, K.; Chen, Y. K.; Liao, P.; Qiu, J. F.; Lin, Y.; Cai, X. F.; Wang, D. Q.; Hu, Y.; Ren, J. H.; Tang, N.; Xu, Y. Y.; Yu, L. H.; Mo, Z.; Gong, F.; Zhang, X. L.; Tian, W. G.; Hu, L.; Zhang, X. X.; Xiang, J. L.; Du, H. X.; Liu, H. W.; Lang, C. H.; Luo, X. H.; Wu, S. B.; Cui, X. P.; Zhou, Z.; Zhu, M. M.; Wang, J.; Xue, C. J.; Li, X. F.; Wang, L.; Li, Z. J.; Wang, K.; Niu, C. C.; Yang, Q. J.; Tang, X. J.; Zhang, Y.; Liu, X. M.; Li, J. J.; Zhang, D. C.; Zhang, F.; Liu, P.; Yuan, J.; Li, Q.; Hu, J. L.; Chen, J.; Huang, A. L. *Nat. Med.* **2020**, *26* (6), 845−848.

(22) Marklund, E.; Leach, S.; Axelsson, H.; Nystrom, K.; Norder, H.; Bemark, M.; Angeletti, D.; Lundgren, A.; Nilsson, S.; Andersson, L.

M.; Yilmaz, A.; Lindh, M.; Liljeqvist, J.; Gisslen, M. *PLoS One* **2020**, *15* (10), e0241104.
(23) Yu, H. Q.; Sun, B. Q.; Fang, Z. F.; Zhao, J. C.; Liu, X. Y.; Li, Y. M.; Sun, X. Z.; Liang, H. F.; Zhong, B.; Huang, Z. F.; Zheng, P. Y.; Tian, L. F.; Qu, H. Q.; Liu, D. C.; Wang, E. Y.; Xiao, X. J.; Li, S. Y.; Ye, F.; Guan, L.; Hu, D. S.; Hakonarson, H.; Liu, Z. G.; Zhong, N. S. *Eur. Respir. J.* **2020**, *56* (2), 2001526.
(24) Ayres, J. S. A. *Nat. Metab.* **2020**, *2* (7), 572−585.
(25) Lim, S.; Bae, J. H.; Kwon, H. S.; Nauck, M. A. *Nat. Rev. Endocrinol.* **2021**, *17*, 11−30.
(26) Pang, Z.; Zhou, G.; Chong, J.; Xia, J. *Metabolites* **2021**, *11* (1), 44.

https://doi.org/10.1021/acs.analchem.1c00596
Anal. Chem. 2021, 93, 10391−10396